Oxidation and Crosslinking Processes During Thermal Aging of Low-Density Polyethylene Films

Salem F. Chabira,[1] Mohamed Sebaa,[1] Christian G'sell[2]

[1]*Laboratoire de mécanique (LME), Université Ammar Telidji, BP 37 G, 03000 Laghouat, Algérie*
[2]*Institut Jean Lamour, UMR 7198 CNRS - Nancy Université, Département Science et Ingénierie des Matériaux et de la Métallurgie, Ecole des Mines de Nancy, Parc de Saurupt, 54042 Nancy, France*

Received 9 May 2010; accepted 3 January 2011
DOI 10.1002/app.34080
Published online 14 December 2011 in Wiley Online Library (wileyonlinelibrary.com).

ABSTRACT: This work analyzes the influence of thermal degradation on the microstructure and the mechanical properties of low-density polyethylene subjected to aging at 70°C in the dark for times up to 21 months. It is found that the polymer shows a gradual increase of its elastic modulus and a dramatic reduction of its ductility, due to secondary crystallization. Infrared spectroscopy (FTIR) reveals the autoaccelerated oxidation of the polymer after 5 months aging. It is observed that the unsaturated vinylidene groups initially present in the material are gradually overridden by vinyl groups and, eventually, by t-vinylene groups. Nuclear magnetic resonance (^{13}C NMR) shows that the initial butyl chain branches are progressively completed by shorter ramifications, namely ethyl branches. These results are discussed in term of macromolecular mechanisms: (i) oxidation, (ii) chain scission, and (iii) crosslinking.
 J Appl Polym Sci 124: 5200–5208, 2012

Key words: low-density polyethylene; thermal aging; mechanical properties; FTIR; ^{13}C NMR

INTRODUCTION

Plastic films for greenhouse covering, when exposed outdoor, under severe conditions in the Sahara degrade through the combined influences of solar radiations, temperature, atmospheric oxygen, humidity, rain, sand wind, and pollutants.[1,2] Not only this degradation is important for practical applications but also it addresses many fundamental problems that deserve to be elucidated in terms of polymer microstructure.

In a previous publication,[3] we analyzed the mechanical properties of low-density polyethylene (LDPE) films exposed to climatic aging under real outdoor exposition in the Saharan area of Laghouat. Essentially, we showed that this exposure made the films stiffer (increase in Young's modulus) and more brittle (decrease in elongation at break). Microstructural investigation of aged films showed that the outdoor weathering induces the formation of hydroperoxides that favors scission of macromolecules and secondary crystallization. Another significant mechanism is the crosslinking of chains that is caused by two main processes: (i) combination of a vinylidene group with a skeleton alkyl, leading to junctions made of two tertiary carbons separated by a CH_2 group and (ii) reaction of secondary alkyls leading to junctions made by a covalent bond joining tertiary carbon atoms. The former process saturates after 4 months of aging, while the latter develops after this delay.

Although, in the latter work, the film samples were subjected to severe solar radiations, we observed that their temperature remained lower than 50°C because of natural air convection. As such, the results published in that article did not take into account the critical situation of film portions situated at contact points with the metallic or wooden frame of a greenhouse, which are susceptible to reach local temperatures up to about 70°C.[3] To analyze the specific influence of temperature in such extreme conditions, we decided to investigate the degradation processes in specimens maintained in the dark at 70°C, following a protocol used previously by several workers.[2,4–7] Under such conditions, we carefully analyzed the decay of mechanical properties versus aging time, and we characterized the evolution of the polymeric microstructure by means of various methods including calorimetric tests (DSC), infrared spectroscopy (FTIR), and nuclear magnetic resonance (^{13}C NMR).

MATERIALS AND METHODS

Material and aging conditions

The LDPE utilized in this investigation is a commercial film produced by the ENIP Company (Skikda,

Correspondence to: S. F. Chabira (s.chabira@mail.lagh-univ.dz).

Algeria) under the reference B24/2. This polymer is a neat grade exempt of stabilizing agents. The melt was extruded at about 175°C and blown in a continuous process characterized by a bubble diameter of 4.4 m, a wall thickness of 180 μm, and a drawing speed of 15 cm/s.

Thermal aging was conducted at 70°C in an oven ventilated with air. Samples were taken out of the oven after prescribed aging times, t_a, ranging from 0 to 21 months, in view of characterizing their properties and microstructure. Beyond 6 months of exposure, the films became too brittle to be mechanically tested. However, their microstructural characterization could be continued after aging times up to 21 months.

Mechanical testing

Tensile tests were run with an Instron 4464 machine according to the NF T54-102 standard with rectangular specimens cut out of the original and aged films. The overall dimensions of the test pieces were 180 mm × 10 mm, with a calibrated portion of initial length $L_0 = 120$ mm, width $w_0 = 10$ mm, and thickness $t_0 = 0.18$ mm. All the tests were conducted at room temperature ($T = 21 \pm 1$°C) at a nearly constant relative humidity ($RH = 50 \pm 5\%$). According to the ISO standard, the results of the tensile tests are presented in terms of the nominal stress, $\sigma = F/(w_0 \times t_0)$ and the nominal strain, $\varepsilon = (L/L_0) - 1$, where F is the tensile force and L the current length of the calibrated portion of the sample. The Young's modulus, E, was determined as the initial slope of the $\sigma(\varepsilon)$ curve. To optimize the duration of the tests, the strain rate was fixed at a low value ($d\varepsilon/dt = 3 \times 10^{-4}$ s^{-1}) until the yield point is passed and then stepped to a higher value ($d\varepsilon/dt = 3 \times 10^{-2}$ s^{-1}) for the rest of the test until fracture occurred. The stress and strain at rupture (σ_r, ε_r) were measured while the sample reached its ultimate elongation before ductile or semibrittle failure occurred.

Microstructural characterization

The degree of crystallinity of the samples was determined in the following way by means of a differential scanning calorimeter (DSC Mettler TA 3000) interfaced with a microcomputer controller. Indium was used for calibration. The samples (about 10 mg in weight) were heated from −150 to 200°C with a heating rate of 10°C/min. The heat of fusion, ΔH_f, was determined after relevant elimination of the base line. The mass-based degree of crystallinity was calculated with reference to the thermodynamic heat of fusion of 100% crystallized polyethylene [$\Delta H_f^c = 285$ J/g (Ref. 8)] by the relationship: $X_c^m = \Delta H_f/\Delta H_f^c$.

Infrared spectroscopy was performed on an FTIR apparatus "Nicolet 210" (now maintained by Bruker). The specific absorption peaks were analyzed from the spectra delivered by the equipment. For each peak, the "optical density" (OD) was determined following the usual definition as $OD = \ln(I_0/I)$, where I_0 is the reference infrared intensity corresponding to the baseline of the spectrum at the peak wave number, and I is the minimum intensity at the bottom of the peak.

NMR spectra were acquired with a high-resolution ^{13}C Bruker DPX apparatus, operating at a frequency of 400 MHz. The specimen glass tube introduced in the apparatus contained a few milligrams of the LDPE films dissolved in deuterated ethylene tetrachloride ($C_2D_2Cl_4$) at 110°C. To distinguish the parity of bonds of carbon atoms, we completed the conventional NMR investigation with the standard Attached Proton Test (APT).[9] In this procedure, the NMR peaks due to evenly bonded atoms (C and CH_2) remain positive, while those due to oddly bonded atoms (CH and CH_3) become negative.

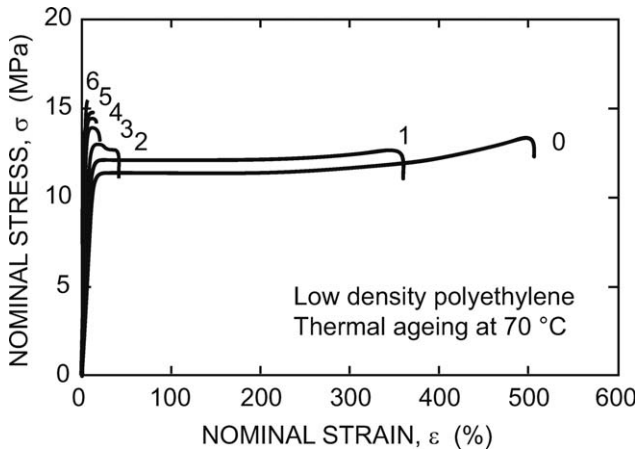

Figure 1 Load versus elongation curves for five stages of aging (0, 1, 2, 3, 4, 5, and 6 months).

EXPERIMENTAL

Mechanical properties

The graph in Figure 1 shows typical stress versus strain curves obtained with films aged at 70°C for increasing times. They demonstrate the dramatic influence of the heat treatment on the mechanical properties of the polymer, namely, (i) elastic stiffening, (ii) increase of yield stress, and (iii) embrittlement. The elastic regime terminates either by plastic deformation or by brittle rupture. The former behavior is principally observed after short aging times (typically $t_a < 2$ months) with a definite drawing stage before the sample tears in a ductile way. For longer aging times (up to 5 months), the stress–strain curves show a short stress drop after yield. Eventually, for $t_a > 5$ months, the material is

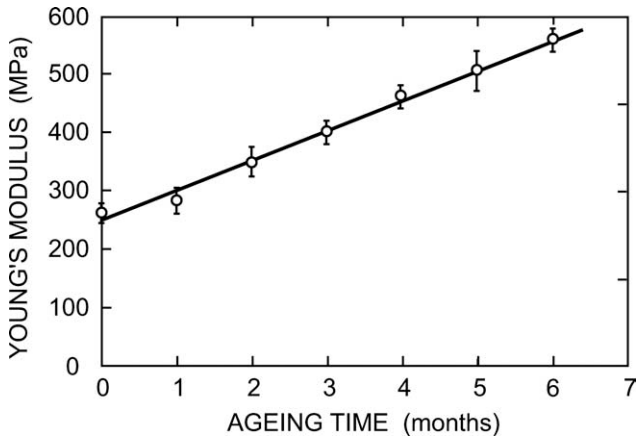

Figure 2 Young's modulus versus aging time.

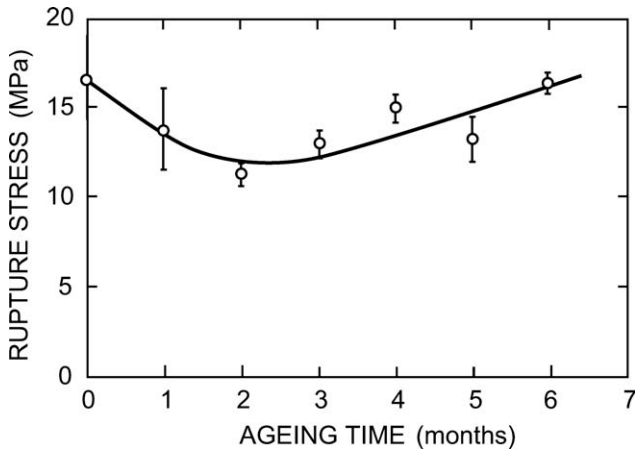

Figure 4 Rupture stress versus aging time.

incapable of undergoing any plastic deformation and the specimens break suddenly in the elastic regime. We will now examine these different points more quantitatively.

The evolution of the Young's modulus, E, is displayed in Figure 2 versus thermal aging time. This curve is almost linear. It starts from 230 MPa and reaches 570 MPa after $t_a = 6$ months, representing a global increase of about 250%.

Like in a previous work,[3] we determined the evolution of strain and stress at rupture versus exposure time. Figure 3 shows that the rupture strain of the material decreases dramatically from about 500% to <20% during the first 2 months of aging. Eventually, after 6 months, it is so brittle that mechanical testing becomes impossible. As for the rupture stress, Figure 4 shows that it decreases during the initial aging period up to 2 months (due to the progressive suppression of the plastic stage) and subsequently increases.

Calorimetric analysis

The DSC curves of the films for different aging times are displayed in Figure 5. The first point deduced from this graph is that the total heat of fusion of the polymer increases during the aging process. Consequently, it is shown (Fig. 6) that the variation of X_c^m follows a linear rate versus t_a, with an initial value as small as 35 wt % for the original LDPE films and reaching 55 wt % after 21 months of aging.

Another information available from the DSC analysis is that the temperature at the top of the fusion peak increases from 117.7 ± 0.1°C up to 120.5 ± 0.5°C after 21 months of thermal aging.

Lastly, we focus our attention onto the left side of the fusion peak. It is important to remark that the temperature at which the aging was performed (70°C) is situated above the lower foot of the broad endotherm (≈60°C) that marks the onset of fusion.[10] Consequently, the growth of X_c^m corresponds to the secondary crystallization of mobile short chain segments coming from the oxidative cleavage of macromolecules.[11,12]

Like previous authors,[13] we consider that the evolution of polymer crystallinity is the key of the increase of Young's modulus. For thermal aging, this relationship is even more evident than for outdoor

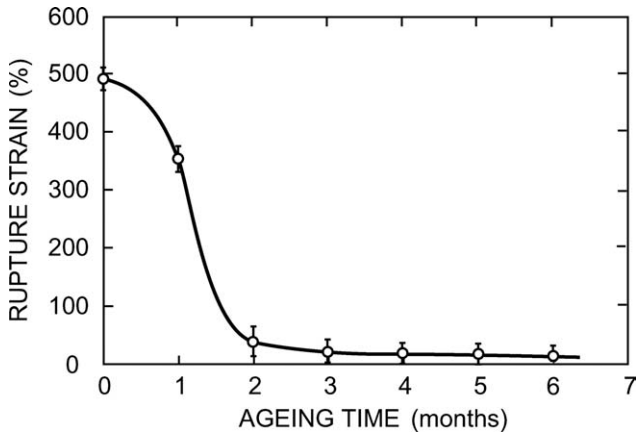

Figure 3 Rupture strain versus aging time.

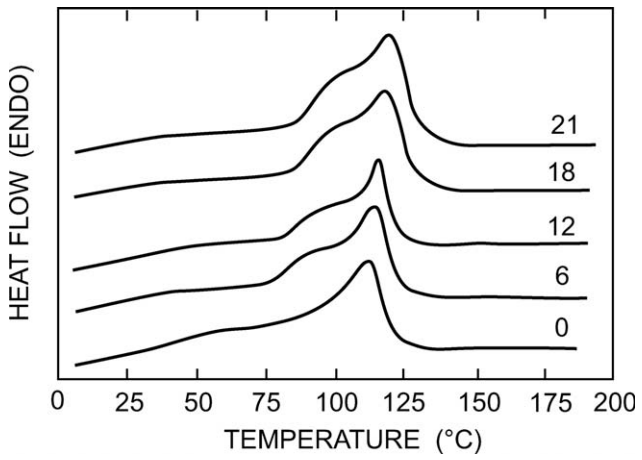

Figure 5 DSC curves for different aging time.

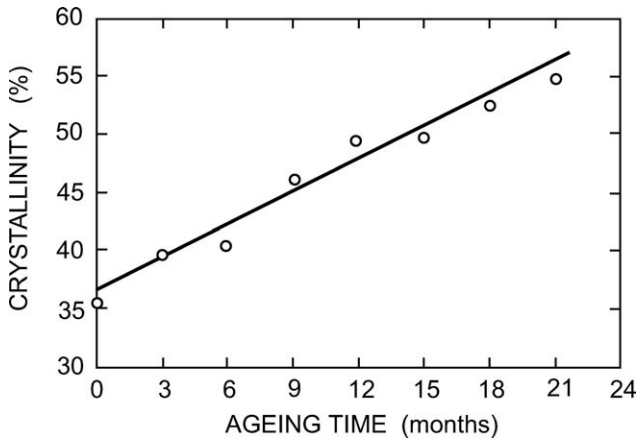

Figure 6 Mass-based crystallinity versus aging time.

aging experiments. Here the aging temperature is an important factor since, as shown in the literature,[14] secondary crystallization of low molecular weight chains is fairly rapid at temperatures $\sim 70°C$.

FTIR characterization

The oxidation process of the LDPE films at 70°C is followed through the growth of the absorption band between 1710 and 1800 cm^{-1} attributed to the carbonyl groups (side oxygen atoms linked to a carbon atom of the chain by a double bond). This IR band is complex with lots of subpeaks and shoulders, due to the multiplicity of oxidation products (carboxylic acids, esters, peresters, peracids, lactones, etc.) The graph in Figure 7 shows that the amplitude of the carbonyl peak at 1712 cm^{-1} presents a typical S-shape evolution versus t_a. This particular feature reflects the progressive oxidation of the LDPE during thermal aging[3]: (i) practically no oxidation during the first 5 months, (ii) steep increase between 5 and 10 months, and (iii) eventual stabilization of the carbonyl concentration.

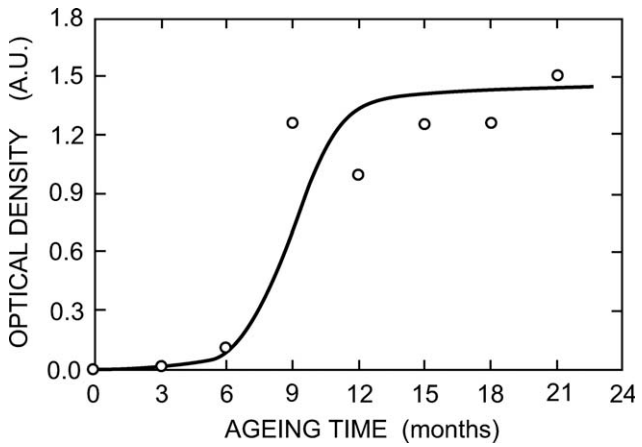

Figure 7 Variation versus aging time of the OD of the IR peak at 1712 cm^{-1} corresponding to carbonyl groups.

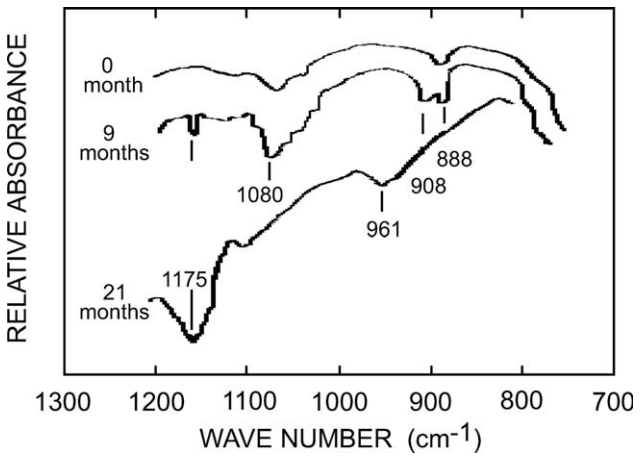

Figure 8 Vinyl species range of the IR spectrum of thermally aged PE film.

Other IR bands, included in the frequency interval between 800 and 1000 cm^{-1}, are also of considerable interest since they correspond to the vibrational bending mode of the vinyl species (Fig. 8). Formation or consumption of a given type of unsaturation gives a good insight on the potential route followed by the photooxidation mechanism.

The starting samples show an absorption band due to vinylidenes ($R_2C{=}CH_2$) at 888 cm^{-1} that corresponds to an unsaturated configuration appearing inherited from the high-pressure polymerization process.[15] The band due to vinyl groups ($RCH{=}CH_2$) at 908 cm^{-1}, absent from the spectrum of the starting film, grows progressively during aging. The t-vinylene (R—CH=CH—R′) peak at 961 cm^{-1}, that is also invisible in the original spectrum, grows so much during the last stages of the aging process that its signals overlaps those of the two previous chemicals species described just above. This indicates that the concentration of t-vinylene exceeds that of the other vinyl species by far. Moreover, the absence of any shoulder or subpeak at the place of the vinyls and the vinylidenes could also suggest that they have been completely consumed during aging.

NMR characterization

The microstructure of the pristine LDPE film has been studied in a previous work.[3] This characterization showed that its molecular structure includes (i) many branches of the butyl type (4 carbon atoms), (ii) a few amyl branches (5 carbon atoms), and (iii) no long chain branches.

Here, we analyze the ^{13}C NMR spectrum of a film after 21 months aging. In the shift range between 10 and 45 ppm [Fig. 9(a)], one sees new chemical shifts at 11.07, 26.69, 25.00, 42.96, and 43.77 ppm, that were invisible in the spectrum obtained with the LDPE before aging. The two first ones are those of

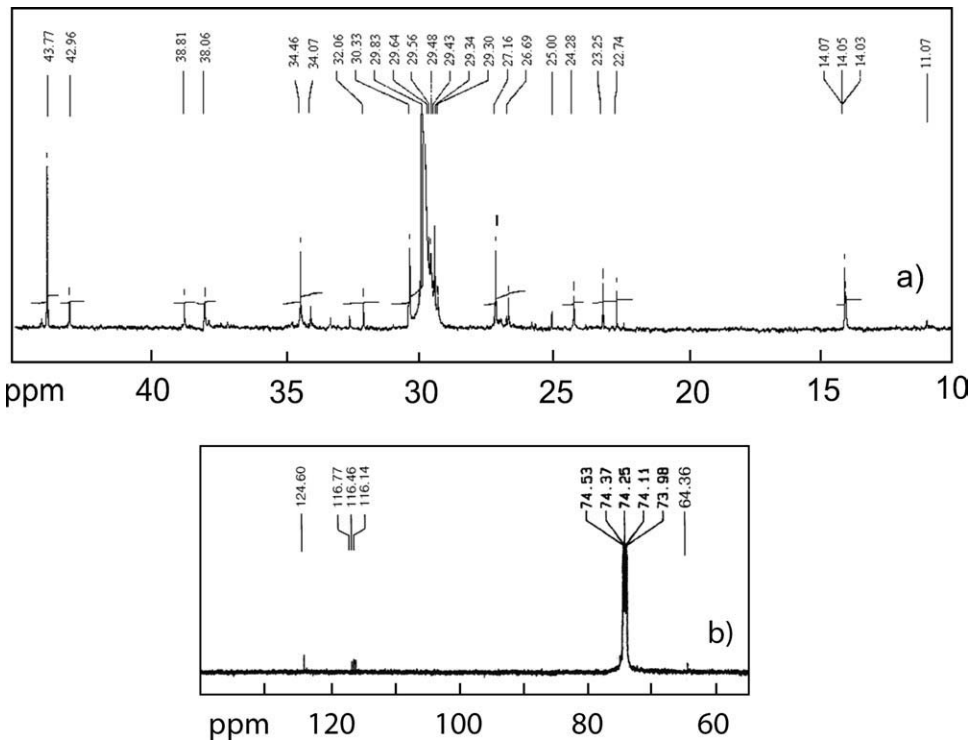

Figure 9 ^{13}C NMR spectrum of a LDPE film after 21 months thermal aging: (a) 10–45 ppm shift range and (b) 60–130 ppm shift range.

ethyl branches identified otherwise in weathered films.[3] The chemical shift at 42.96 ppm is probably that of quaternary carbons. The observation that the signal remains positive when analyzed by APT confirms this assumption.

The formation of crosslinks probably results of the radial combination of two tertiary alkyl radicals, leading to the formation of quaternary carbon atoms. The chemical shifts at 25.00 and 43.77 ppm are assigned to carbonyl groups, specifically to α and β carbons, respectively.[16,17] These resonances, that appear strongly in the spectra of thermally aged polyethylene films, where previously ascribed to their high degree of oxidation.[18] Another range of the same NMR spectrum, from 60 to 130 ppm, is displayed in Figure 9(b). Here, again new peaks appear at 116.14, 116.46, 116.77, and 124.60 ppm. They are significant despite their low intensity. The three chemical shifts centered by 116.46 ppm are typical to vinyl carbons. The peak at 124.60 ppm is assigned to t-vinylene groups. This confirms the IR evidence of the high concentration of t-vinylidene groups in thermally aged films.

DISCUSSION

Influence of microstructural changes on the mechanical properties

The analysis of the broad fusion peak recorded in the DSC tests gives some indications how the short chain segments produced by the chain scission process contribute to the linear increase of crystallinity recorded with time during the total duration of the heat treatment (Fig. 6). In that scope, two secondary crystallization mechanisms can be envisaged: (i) incorporation into existing crystallites and (ii) nucleation of new crystallites.

The first mechanism should increase significantly the thickness of the lamellae present in the original films. Actually, we remarked that the temperature at the fusion peak increases somehow with the aging time. However, by applying the classical Gibbs–Thomson model with the characteristic thermodynamic parameters of polyethylene published by Wunderlich,[8] we find that the thickness of the corresponding lamellae increases moderately (from 11.3 ± 0.5 nm in the original state to 12.7 ± 0.5 nm after 21 months at 70°C). Also the amplitude of the main fusion peak shows a limited increase (about 15%) with the aging time.

The second mechanism, for its part, is likely to generate an increasing population of thin lamellae. It is evident that, in the DSC curves of the aged films, a definite shoulder develops more and more on the left side of the fusion peak. The characteristic temperature of this shoulder is about 95°C after 6 months aging and 105°C after 21 months. These values correspond to lamella thickness of 5.8 ± 0.5 nm and 7.4 ± 0.5 nm, respectively. Furthermore, it is noted that the amplitude of the shoulder increases dramatically during the aging process.

From the arguments presented above, we consider that the nucleation of new crystallites plays a major role in the increase of X_c^m and, in turn, the gradual increase of the Young's modulus displayed in Figure 2. By contrast, the growth of pre-existing crystallites plays a minor role in the secondary crystallization process and in the stiffening of the material.

Also it is interesting to recall that for outside weathering with solar irradiation, we found previously[3] a nonlinear increase of crystallinity and a significant saturation of the Young's modulus after 4 months of exposure. This difference is probably due to the fact that, in the weathering experiments, the local temperature within the material did not exceed 50°C.

However, the most dramatic phenomenon in thermally aged films is the loss of ductility of the material (the deformation at break decreases from 500% to 20% within an aging time of about 2 months). This degradation is due to the formation of free radicals, macroperoxy radicals and eventually chain scissions in the macromolecules, as shown by microstructural characterization. Since the LDPE is a semicrystalline polymer with a glass transition temperature far below ambient, the toughness of the material is controlled by the efficiency of the tie molecules that link neighboring crystallites across the amorphous phase. Consequently, these molecules are particularly vulnerable to chain scission under the effect of oxygen that diffuses rapidly within the disordered amorphous interstices. We postulate that the sharp ductile-to-brittle transition experienced by the material corresponds to the aging time when the fraction of damaged tie molecules reaches a critical value. What is not completely clear at this point is the distribution of damage processes throughout the film thickness. Oxidation of the films is certainly more active near the surface than in the core. Owing to this fact, fracture should be nucleated from defects (crazes, etc.) more likely situated at the film surface.

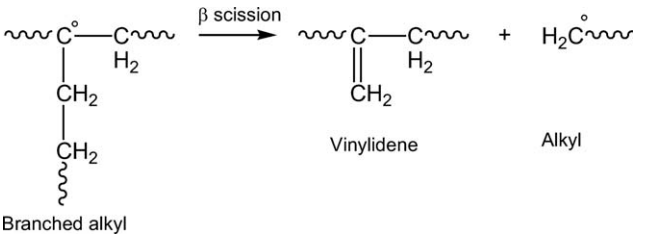

Figure 10 β scission of an alkyl leading to the formation of vinylidene species (888 cm^{-1}).

General analysis of the degradation mechanisms

In this section, we discuss the chemical mechanisms that induce the degradation of the LDPE film while they are subjected to thermal aging. This analysis, of the same vein as that published in our recent article on the effects of natural weathering,[3] aims understanding more precisely the free radical propagation processes that govern the thermooxidative degradation of LDPE.[19] Here, we examine which mechanisms are active in both protocols and which ones are specific to the thermal aging.

Following previous authors,[4,11,20,21] it can be stated that, for most polymers, the generic oxidation mechanism that controls both radiation and thermal aging is the so-called "Boland mechanism" that acts in three stages: initiation, propagation, and termination. In the initiation stage, the radiation and/or thermal energy causes the abstraction of a hydrogen atom from a polymeric chain. The macroradical (R°) thus created reacts with the surrounding oxygen to form a peroxide (ROO°). In the propagation stage, the peroxide abstracts another hydrogen atom from a polymeric chain to constitute a hydroperoxide (ROOH). Eventually in the termination stage, the different radicals combine together to form a variety of products such as ketones (R═O), hydroperoxides (R—OOH) alkyl chains (R—R), esters (RC(O)—OR), etc.

FTIR characterization showed that the final oxidation products, resulting from the termination reactions, are the same for radiation and thermal aging. They are mainly aldehydes, ketones, carboxylic acids, peresters, peracids, γ-lactones, etc. However, careful analysis of IR spectra shows that the routes followed by the macroradicals during the propagation stage are not exactly the same in the two aging conditions, particularly to what is concerned with the vinyl species that develop much faster during thermal aging. Consequently, it is logical that the drop of the mechanical toughness were more dramatic in the latter protocol.

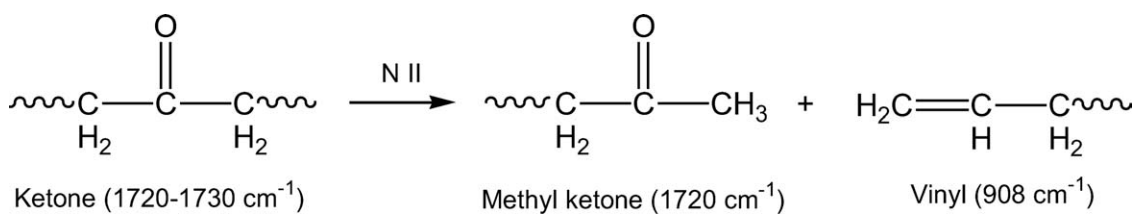

Figure 11 Norrish type II reaction transforming a ketone into a chain end ketone and a vinyl group.

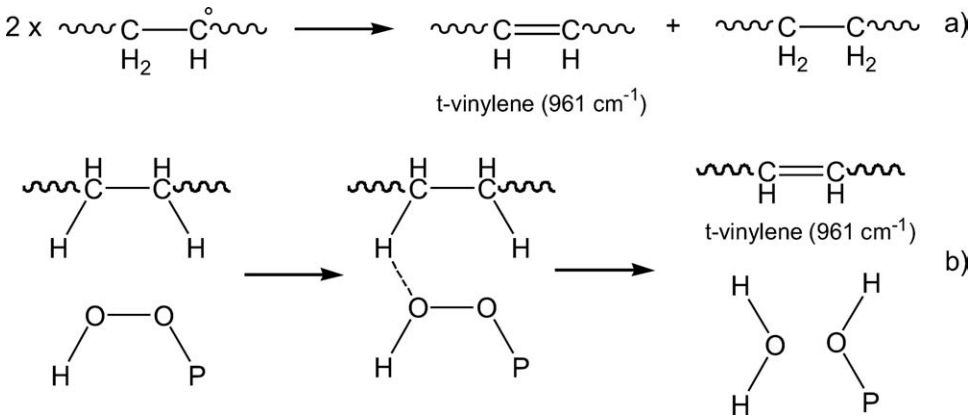

Figure 12 Two different routes of vinylidenes formation: (a) disproportionation reaction and (b) bimolecular reaction.

The oxidation kinetic is somewhat singular and follows an S-shaped curve, which shows clearly that oxidation occurs in three distinguishable stages. The first one corresponds to an induction period, which is relatively longer for thermal aging than under solar irradiation.[3] The average rate of oxidation during this period (i.e., 0–6 months) is $d(O.D.)/dt \approx 0.018$ month^{-1}. After the oxidation products have reached a critical threshold concentration, an autoaccelerated oxidation process follows with an average rate of $d(O.D.)/dt \approx 0.238$ month^{-1}, which lasts for a relatively short period of time, about 6 months. The final stage, which starts after 12 months, is a plateau where the average rate of oxidation $d(O.D.)/dt \approx 0$ month^{-1}.

The above results indicate that thermal aging is less severe than radiation aging for the initiation of oxidation. By contrast, heating is more efficient than irradiation for the homolytic cleavage of covalent bonds responsible for the early loss of the mechanical properties.

Role played by vinyl species in the thermodegradation process

As shown previously,[3] radiation aging activates the progressive exhaustion of vinylidenes (888 cm^{-1}) by reaction with alkyl radicals and provokes the crosslinking of macromolecules. In turn, the latter process induces a certain consolidation of the material. By contrast, during thermal aging in the dark, a small but significant increase of the vinylidene concentration is observed (Fig. 8). Like others,[22,23] we propose that this increase may result from the β scission of tertiary alkyl radicals leading to the formation of vinylidene and chain alkyl radicals, as depicted in Figure 10.

Like the radiation aging protocol, thermal aging causes the continuous production of vinyl groups (908 cm^{-1}). They result from chain scission reactions occurring in the proximity of carbonyl groups via the well-known Norrish type II reaction process (Fig. 11).[1,3,4,24,25]

At an advanced stage of the aging protocol, the trans-vinylene groups (961 cm^{-1}) are the most numerous species among the vinyls present in the specimens. This type of unsaturations can be produced via two different routes: (i) The first one implies the disproportionation of skeleton alkyls produced by the abstraction of hydrogen atoms from the main chain [Fig. 12(a)] and (ii) the second one, also reported in the literature,[1,25,26] consists in the bimolecular reaction between a hydroperoxide and a chain segment of the polymer [Fig. 12(b)].

The variation of the IR band of the vinyl species has highlighted the important role played by the unsaturated groups in the weakening of the material through the promotion of chain scission reactions. While the vinylidenes favor material consolidation during radiation aging, they cause its early weakening during thermal aging.

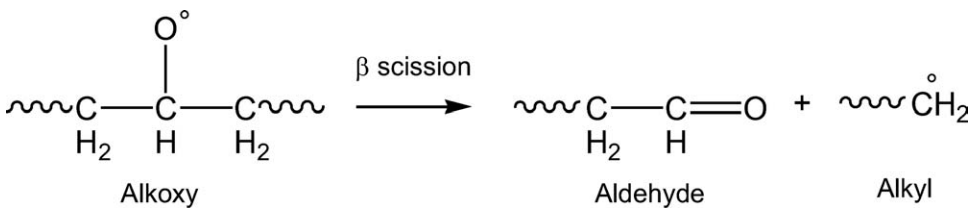

Figure 13 β scission of an alkoxy.

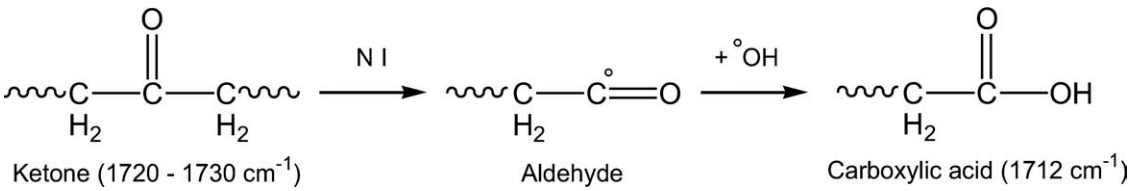

Figure 14 Norrish type I reaction transforming a ketone into a carboxylic acid.

Other aspects of the thermochemical molecular degradation

The vinyl groups are not the only chemical indicators of the decrease of the average molecular weight via a chain scission process. Other chemical structures such as hydroperoxides, carbonyls and various free radicals coming from bond cleavage or hydrogen abstraction, contribute significantly to the degradation of the molecular structure. These mechanisms are now reviewed.

Atmospheric oxygen atoms, which easily diffuse into the LDPE at elevated temperatures, are responsible for the oxidation of the thermally aged polymer through the formation of hydroperoxides, via a mechanism similar to the thermal oxidation of the polymer during processing.[19] Subsequent decomposition of hydroperoxides into free radicals plays a key role in the weakening of the films. The resulting alkoxy radical being instable at elevated temperature undergoes a β scission leading to the formation of an aldehyde and a free alkyl radical. This reaction (Fig. 13) is known to be very efficient at elevated temperature.[7,18,27,28]

The very high concentration of carboxylic acids indicate that chain scission reactions via the Norrish type I process play also an important role in weakening the films (Fig. 14). The chain scission reactions causing notably the elimination of the long chains, we consider that this mechanism is responsible of the material embrittlement.

By contrast to outdoor aging that imposes severe mechanical stresses to the samples (particularly because of desert winds), thermal aging respects the film integrity even after the onset of embrittlement. This allowed us to follow the infrared and NMR peaks during 21 months of thermal aging and particularly the fast multiplication of carbonyl groups between 6 and 12 months. The NMR spectroscopy was sensitive enough to detect the chemical shift of the α and β carbons of ketone groups at 25.00 and 43.77 ppm, respectively (Fig. 15). As for the IR spectra, the S-shaped evolution of the carbonyl peak at 1712 cm^{-1} (Fig. 7) proves that the oxidation kinetics becomes an autoaccelerated process, which saturates after 12 months.

During the last stage of aging, the films show a significant consolidation, which is ascribed to chain crosslinking. This mechanism is probably due to the presence of tertiary carbon atoms that favor the chemical vulnerability of polymeric chains, particularly to what is concerned with the hydrogen abstraction from carbon atoms situated at the root of a lateral branches (C_{br} atoms). The resulting tertiary alkyl radicals recombine together via the construction of a covalent bond between C_{br} atoms of two neighboring chains (Fig. 16). This leads to a new molecular structure constituted by quaternary carbon atoms.

Among the different crosslinking mechanisms described previously,[3] the most probable in thermal aging seems to be the one proposed below. The junction of the tertiary radicals by a covalent bond leads to quaternary atoms characterized by the NMR peak at 42.96 ppm. The formation of quaternary carbon atoms during thermal aging is an effective but rather late process. However, in the present case, it does not seem to be efficient enough to improve the polymer toughness as shown by the drastic reduction of the rupture strain on aging. This is because the positive effect of crosslinking is overridden by other damage mechanisms due to polymer oxidation. From the observation that LDPE have lost 50% of its original rupture strain after only 1 month of thermal aging at 70°C (Fig. 3), it s clear that temperature is a major parameter in the overall damage rate of LDPE subjected to radiation or thermal aging.[4]

CONCLUSIONS

The exposure of LDPE films for greenhouse covering in the very hostile environment of Sahara leads to a dramatic loss of their mechanical performances. The aging kinetic is particularly serious at the contact points with the metallic or wooden frame of the greenhouse because local heating can bring the temperature up to 70°C in such zones. To investigate the specific effect of temperature on polymer degradation, LDPE films specimens were kept in the dark

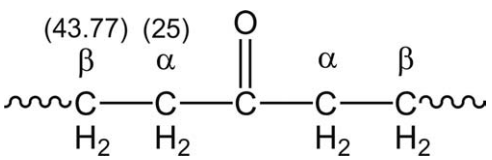

Figure 15 Carbonyl structure in thermally aged polyethylene.

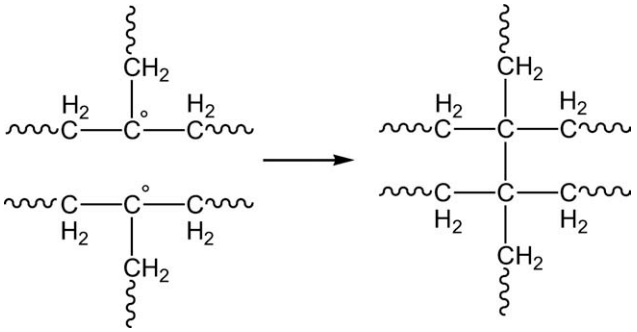

Figure 16 Formation of a crosslink between two polymeric chains with tertiary alkyls via the formation of quaternary carbon atoms.

at that temperature during increasing times up to 21 months, while the mechanical properties and molecular microstructure were carefully analyzed.

The selected aging temperature being above the lower foot of the melting endotherm (about 60°C), a progressive increase of crystallinity is observed during the aging time. This secondary crystallization is mainly due to the nucleation of new crystallites with short chain segments issued from chain scissions and, to a lesser extent, to the incorporation of these chain segments into existing crystallites. This effect causes an almost linear increase of the Young's modulus. The chain scission process is also responsible for the abrupt drop of the rupture strain that is observed very early during the thermal aging protocol. We have analyzed three mechanisms potentially responsible for chain scissions in LDPE. The first one consists of the β scission of tertiary alkyl radicals leading to the formation of vinylidene species. The second one is the β scission of an alkoxy radical leading to the formation of an aldehyde and an alkyl radical. The third one is the Norrish type I process that transforms ketone groups to aldehydes and ultimately to carboxylic acids. We showed that the latter mechanism is the most important one.

Furthermore, the C^{13} NMR spectroscopy reveals the presence of quaternary carbon atoms in the highly degraded films, which indicates the formation of crosslinks that result from the reaction of tertiary alkyls situated in neighboring chains. However, the crosslinks play only a secondary role and are incapable, per se, to ensure a sufficient elongation at break when they are in concurrence with the chain scissions processes. Consequently, covering greenhouses in Saharan sites represents a difficult challenge since the lifetime of LDPE film is limited by its microstructural damage at the contact points with the frame.

References

1. Mendes, L. C.; Rufino, E. S.; Filipe de Paula, O. C.; Torres, A. C., Jr. Polym Degrad Stab 2003, 79, 371.
2. Verdu, J. Plast Mod Elastom 1973, 25, 125.
3. Chabira, S. F.; Sebaa, M.; G'sell, C. J Appl Polym Sci 2008, 110, 2516.
4. Verdu, J. Vieillissement des Plastiques; Afnor Eyrolles: Paris, 1984.
5. Fayolle, B.; Colin, X.; Audouin, L.; Verdu, J. Polym Degrad Stab 2007, 92, 231.
6. Qureshi, F. S.; Amin, M. B.; Maadhah, A. G.; Hamid, S. H. Polym Plast Technol Eng 1989, 28, 649.
7. El Awady, M. M. J Appl Polym Sci 2003, 87, 2365.
8. Wunderlich, B. Macromolecular Physics, vol. 1: Crystal structure, morphology, defects; Academic Press: New York, 1973.
9. Silverstein, R. M.; Basler, R. C.; Morill, T. C. Identification Spectrométrique de Composés Organiques; Boeck Université: Paris and Brussels, 1998.
10. Carlsson, D. J.; Bazan, G.; Chmela, S.; Wiles, D. M.; Russell, K. E. Polym Degrad Stab 1987, 19, 195.
11. Hawkins, W. L. Polym Eng Sci 1964, 4, 187.
12. Gugumus, F. Angew Makromol Chem 1990, 182, 85.
13. Gulmine, J. V.; Janissek, P. R.; Heise, H. M.; Akcelrud, L. Polym Degrad Stab 2003, 79, 385.
14. Birkinshaw, C.; Buggy, M.; Daly, S.; O'Neill, M. Polym Degrad Stab 1988, 22, 285.
15. Severini, F.; Gallo, R.; Ipsale, S.; Del Fanti, N. Polym Degrad Stab 1986, 14, 341.
16. Seong, O. H.; Dong, W. L.; Oc, H. H. Polym Degrad Stab 1999, 63, 237.
17. Han, O. H.; Chae, S. A.; Han, S. O.; Woo, S. K. Polymer 1999, 40, 6329.
18. Cheng, H. N.; Schilling, F. C.; Bovey, F. A. Macromolecules 1976, 9, 363.
19. Wiles, D. M.; Carlsson, D. J Polym Degrad Stab 1980, 3, 61.
20. Corrales, T. F.; Catalina, C.; Peinado, N. S.; Allen, E.; Fontan, E. J Photochem Photobiol A: Chemistry 2002, 147, 213.
21. Lincoln-Hawkins, W. Polym Eng Sci 1965, 5, 196.
22. Bremner, T.; Rudin, A. J Appl Polym Sci 1995, 57, 271.
23. Valadez-Gonzalez, A.; Cervantes-Uc, J. M.; Veleva, L. Polym Degrad Stab 1999, 63, 253.
24. Tidjani, A. Polym Degrad Stab 2000, 68, 465.
25. Rui, Y.; Jian, Y.; Ying, L.; Kunhua, W. Polym Degrad Stab 2005, 88, 333.
26. Gugumus, F. Polym Degrad Stab 1990, 27, 19.
27. Changqing, J.; Christensen, P. A.; Egerton, T. A.; Lawson, E. J.; White, J. R. Polym Degrad Stab 2006, 91, 1086.
28. Costa, L.; Luda, M.; Trossarelli, L. Polym Degrad Stab 1997, 58, 41.